Virchows Arch (2011) 459:399–407
DOI 10.1007/s00428-011-1120-z

ORIGINAL ARTICLE

Specific expression of ZO-1 and *N*-cadherin in rosette structures of various tumors: possible recapitulation of neural tube formation in embryogenesis and utility as a potentially novel immunohistochemical marker of rosette formation in pulmonary neuroendocrine tumors

Kaishi Satomi · Yukio Morishita · Shingo Sakashita · Yuzuru Kondou · Shuichiroh Furuya · Yuko Minami · Masayuki Noguchi

Received: 19 March 2011 / Revised: 29 June 2011 / Accepted: 4 July 2011 / Published online: 23 July 2011

Abstract Neuroendocrine tumors can develop in various organs. All of these tumors are designated on the basis of their morphologic characteristics evident by light microscopy, and by immunohistochemistry for antigens such as synaptophysin, chromogranin-A, and CD56/NCAM. In the present study, we attempted to demonstrate the localization of Zonula occludens-1 (ZO-1) and *N*-cadherin in rosette structures of neuroendocrine tumors using immunohistochemistry and to clarify their specific distribution in rosettes in human pulmonary neuroendocrine tumors in comparison with various types of adenocarcinoma. Among 40 neuroendocrine tumors of the lung examined, 18 cases (45%) and 22 cases (55%) were positive for ZO-1 and *N*-cadherin, respectively. In addition, we divided the cases into two types: 16 cases of Flexner-type tumor and 24 cases of Homer–Wright-type tumor. We then determined the Rosette Index (RoI; the percentage fraction of rosette structures positive for ZO-1 or *N*-cadherin among the total number of rosette structures). The Flexner-type neuroendocrine tumors showed significantly higher levels of RoI in ZO-1 than the Homer–Wright-type neuroendocrine tumors (median; 38.8% vs 0%, $p<0.001$). On the other hand, *N*-cadherin and ZO-1 were hardly detected in tubular adenocarcinomas in various organs, and their immunoreactivities differed significantly between adenocarcinoma and pulmonary neuroendocrine tumor (ZO-1, mean 0.23% vs 18%, $p<0.0001$; *N*-cadherin, mean 0% vs 33%, $p<0.0001$). In conclusion, expression of ZO-1 and *N*-cadherin may reflect the mechanisms leading to rosette formation in neuroendocrine tumors, which possibly recapitulate neural tube formation in embryogenesis and could represent a specific immunohistochemical marker for neuroendocrine carcinoma of the lung.

Keywords ZO-1 · *N*-cadherin · Neuroendocrine carcinoma · Endocrine carcinoma · Carcinoid · Lung

K. Satomi · Y. Morishita · S. Sakashita · Y. Minami · M. Noguchi (✉)
Department of Diagnostic Pathology, Graduate School of Comprehensive Human Sciences, University of Tsukuba, 1-1-1 Tennodai,
Tsukuba-shi, Ibaraki 305-8575, Japan
e-mail: nmasayuk@md.tsukuba.ac.jp

Y. Kondou · S. Furuya
Department of Pathology, Tsukuba University Hospital, 2-1-1 Amakubo,
Tsukuba-shi, Ibaraki 305-8576, Japan

Introduction

Neuroendocrine tumors of the lung are subdivided into four entities, including typical and atypical carcinoid tumors, small cell lung carcinoma (SCLC) and large cell neuroendocrine carcinoma (LCNEC) [1, 2]. Among these tumors, carcinoids are considered to be relatively indolent, whereas SCLC and LCNEC are thought to be highly aggressive [3–13].

Neuroendocrine tumors can develop in a variety of organs, including the digestive system, endocrine system, urogenital system, and soft tissues [14]. All of these tumors

are classically designated as neuroendocrine tumors on the basis of their characteristic morphological features, including organoid, trabecular, palisading, or rosette growth patterns (Fig. 1). As well as these light-microscopical morphologic characteristics, dense-core neurosecretory vesicles evident by electron microscopy are helpful for diagnosis. Recently, immunohistochemistry, particularly for synaptophysin, chromogranin-A, and CD56/NCAM, has been applied successfully to identify neuroendocrine features. Among the various morphological and immunohistochemical markers, the characteristic morphological feature of rosette formation is strongly pathognomonic, but the molecular mechanism responsible for rosette formation, or its biological significance, is still unclear.

Rosette structures are a very useful morphological marker of neuroendocrine differentiation and are divided into two types: the Flexner type and the Homer–Wright types [15] (Fig. 1). The rosette structure appears as a radial arrangement of tumor cells resembling a rose. The Flexner-type rosette is a spoke- and wheel-shaped tumor cell formation with lumina, which is frequently detected in ependymoma, retinoblastoma, and immature teratoma (Fig. 1a). The Homer–Wright rosette is a circular or spherical grouping of tumor cells around a pale, eosinophilic, central area but lacking lumina, which is typically seen in medulloblastoma and neuroblastoma (Fig. 1b).

On the other hand, embryologically, neural differentiation is characterized by development of the neural tube. Since the morphological structure of the rosette in pulmonary neuroendocrine tumors mimics that of the neural tube, we have hypothesized that rosette structures within neuroendocrine tumors recapitulate the early stage of neural tube formation.

Various proteins are known to be components of the neural tube/neural rosette structure: PAX6, nestin, Sox1, Sox2, and *N*-cadherin as constitutive proteins of neuroepithelium, or PLZF, DACH1, MMRN1, PLAGL1, NF2F1, DMTR3, LMO3, FAM70A, EVI1, ZNF312, LIX1, RSPO3, Shroom-3, and Zonula occludens-1 (ZO-1) as proteins that are associated with the development of neural tube/neural rosette structure [16–19]. Among these molecules, ZO-1 and *N*-cadherin show characteristic localization, especially in early-stage neural rosettes that develop from human embryonic stem cells [17].

N-cadherin, also known as cadherin 2, is a member of the cadherin family. *N*-cadherin is also known to be present, and to accumulate, in the adherens junctions of the apical portion of neuroepithelial cells in chick and mouse embryos [20, 21]. In human tumors, *N*-cadherin is differentially expressed in pulmonary tumors and is observed predominantly in neuroendocrine lung lesions, neuroendocrine hyperplasia, typical carcinoid tumor, atypical carcinoid tumor, SCLC and LCNEC. Neuroendocrine hyperplasia, typical carcinoid, small cell lung carcinoma, and large cell neuroendocrine carcinoma demonstrate diffuse membranous *N*-cadherin immunoreactivity, whereas atypical carcinoid exhibits strong and diffuse and membranous immunoreactivity [22].

ZO-1, also known as tight junction protein 1, is a 225-kDa tight junction-associated polypeptide [23]. It is not only concentrated at tight junctions in epithelial cells but also colocalized with the cadherin molecule in non-epithelial tissue [24]. Since ZO-1-deficient mice show a lethal embryonic phenotype, it is thought that ZO-1 plays essential roles in development [25, 26].

It is also known that expression of ZO-1 is maintained both before and after closure of the neural tube in both chick and mouse neuroepithelium [18]. In human embryonal stem cells (hESCs), the formation of neural rosettes is initiated by acquisition of cell polarity, as demonstrated in vitro by redistribution of ZO-1 in the apical membrane, being expressed evenly on the surface of undifferentiated

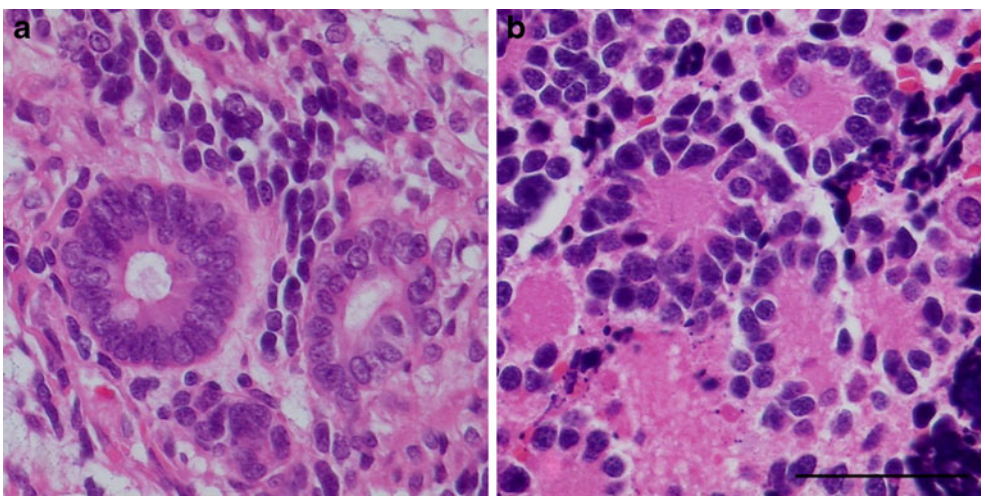

Fig. 1 Histological evaluation of tumor type with rosette structures. Rosette structures distinguished as arrangements of several polarized cells. The Flexner-type rosette in retinoblastoma contains lumina (**a**), while the Homer–Wright-type rosette in neuroblastoma does not (**b**). We defined tumors as the Flexner-type (in which rosettes with lumina are predominant) or the Homer–Wright-type (in which rosettes without lumina are predominant). Scale *bar* 50 μm

hESCs [17]. These reports indicate that ZO-1 is colocalized with *N*-cadherin and plays an important role in neurogenesis.

In the present study, we attempted to clarify the mechanisms leading to rosette formation in neuroendocrine tumors with reference to neural tube formation during embryogenesis using ZO-1 and *N*-cadherin as key proteins of neuroendocrine tumor rosette structures and demonstrated the specific distribution of the two proteins in rosettes of human pulmonary neuroendocrine tumors. Our findings suggested that ZO-1 and *N*-cadherin are useful immunohistochemical markers for clarifying the biological significance of rosette structures, as well as being a diagnostic feature of neuroendocrine tumors.

Materials and methods

Patients and tissue specimens

A total of 101 specimens that had been surgically resected at Tsukuba University Hospital (Ibaraki, Japan) between 1975 and 2009 were retrieved. Written informed consent had been obtained from the patients between 1996 and 2009. All of the cases examined were anonymized, and this study was approved by the institutional review board of the University of Tsukuba. Among these cases, 58 showed rosette formation, including two medulloblastomas, one ependymoma, three neuroblastomas, one olfactory neuroblastoma, two retinoblastomas, two immature teratomas, one mature teratoma, one pineoblastoma, one neurocytoma, one atypical carcinoid of the colon, one atypical carcinoid of the thymus, five typical carcinoids of the lung, two atypical carcinoids of the lung, 25 large cell neuroendocrine carcinomas of the lung, eight small cell carcinomas of the lung, and two large cell carcinomas of the lung. The remaining 43 cases were well-differentiated tubular adenocarcinomas, including three adenocarcinomas of the lung, ten adenocarcinomas of the stomach, ten adenocarcinomas of the colon, five adenocarcinomas of the pancreas, five adenocarcinomas of the bile duct, and ten ductal carcinomas of the breast.

Immunohistochemistry

For immunohistochemical analysis, the following antibodies were used as primary antibodies: anti-*N*-cadherin (6 G11, mouse monoclonal, Dako, Copenhagen, Denmark), anti-ZO-1 (epitope; residues 463–1109 of ZO-1, rabbit polyclonal, Zymed Laboratories, San Francisco, USA), anti-synaptophysin (27 G12, mouse monoclonal, Nichirei Bioscience, Tokyo, Japan), anti-chromogranin-A (A0430, rabbit polyclonal, Dako), and anti-CD56/NCAM (1B6, mouse monoclonal, Nichirei Bioscience).

All specimens had been previously fixed in 15% formalin and paraffin-embedded. Serial sections of the materials were cut at a thickness of 3 μm. Slides were deparaffinized in xylene and dehydrated in methanol. The EnVision® (Dako) signal enhancement system was employed for analysis of all antibodies. Heat-mediated antigen retrieval was used for visualization of *N*-cadherin, synaptophysin (pressure pan treatment, 15 min at 105°C), chromogranin-A, and CD56/NCAM (autoclave treatment, 10 min at 120°C), and an enzymatic antigen retrieval method employing Dako proteinase K Ready-to-use was adopted for ZO-1 (5 min at room temperature; Dako). Tissues were incubated with ChemMate POD Blocking Solution (Dako) for 5 min at room temperature. After blocking, the sections were incubated with the primary antibody diluted in Dako REAL Antibody Diluent (Dako) for 30 min at room temperature. Dilutions used for the primary antibodies were: *N*-cadherin and ZO-1, 1:50; chromogranin-A, 1:500; synaptophysin and CD56/NCAM, pre-diluted. Tissues were washed in TBS and incubated with ENVISION+Dual Link Polymer (Dako) for 30 min. Visualization was performed by incubation with the DAB+ Liquid System (Dako) for 5 min. After being rinsed in water, the sections were counterstained with hematoxylin and mounted. These immunohistochemical processes were performed with a histostainer (Nichirei Biosciences).

The positive controls for immunohistochemistry were liver tissue for anti-*N*-cadherin, normal bronchiole epithelium for anti-ZO-1, and pancreatic islet tissue for anti-synaptophysin, anti-chromogranin-A, and anti-CD56/NCAM.

Evaluation of rosette structure types

Rosette structures can be distinguished as arrangements of several polarized cells. In this study, we distinguished the tumor type as Flexner-type tumors (in which rosette structures with lumina are predominant and correspond to the Flexner type) or Homer–Wright-type tumors (in which rosette structures without lumina are predominant and correspond to the Homer–Wright type; Fig. 1a, b). If any individual case included both types of rosette structure, it was classified according to the predominant type present.

Evaluation of immunostaining

Immunoreactivity in the cytoplasm and/or cell membrane of neural tube-like structures in immature teratoma was classed as negative or positive for *N*-cadherin. On the other hand, immunoreactivity that was evident as apical membrane staining or dot-like positivity in the center of the structure was evaluated as ZO-1 positivity. We used the Rosette Index (RoI) for evaluating the quantity of the rosette structures expressing each of the proteins. The RoI

is defined as the percentage of positive rosette structures among the total in each tumor. We counted 100 rosette structures in each tumor. We considered specimens to be negative for ZO-1 or *N*-cadherin if the RoI score was less than 5%. All histological evaluations were judged by three pathologists (KS, SS, and YK), each of whom examined the RoI score independently without any information, and a 10% score difference was tolerated. If the evaluations differed by over 10%, the pathologists discussed the case, and a consensus diagnosis was reached.

Statistical analysis

Statistical analysis was performed with the SPSS 9.0 software package (SPSS Inc., Chicago, IL, USA). Mann–Whitney *U* test was applied for assessment of anti-ZO-1 positivity as a parameter of RoI. Fisher's exact test was performed for analysis of patient profiles. For all analyses, a significance level of $p<0.05$ was adopted.

Results

Patient background

Among the 40 neuroendocrine tumors of the lung, including five typical carcinoid tumors, two atypical carcinoid tumors, 25 large cell neuroendocrine carcinomas, and eight small cell carcinomas, the clinicopathological characteristics including gender ($p=0.230$, $p=0.180$), pathological stage ($p=0.550$, $p=0.312$), lymphatic duct invasion (Ly factor; $p=0.842$, $p=0.816$), vascular invasion (V factor; $p=0.822$, $p=0.218$), and lymph node status (N factor; $p=0.071$, $p=0.836$) did not show any significant difference between cases positive and negative for both ZO-1 and *N*-cadherin.

Neuroendocrine tumors of the lung and other tumors with rosette structures

The results of immunohistochemical staining in neuroendocrine tumors of the lung and other tumors with rosette structures (total 58 cases, described in "Materials and methods") are summarized in Table 1. Rosette structures are observed in various tumors: neuroblastoma (Fig. 2a), immature teratoma (Fig. 2b), large cell neuroendocrine carcinoma of the lung (Fig. 2c), and small cell carcinoma of the lung (Fig. 2d). Cytoplasmic and/or cell membrane staining for *N*-cadherin were evident in these tumors (Fig. 2 e–h). Among the cases positive for *N*-cadherin, 18 (49%) showed a strong diffuse (cytoplasmic and cell membrane) staining pattern, and only 19 (51%) showed a strong cell membrane staining pattern. *N*-cadherin immunoreactivity was evident not only in rosette structures but also other tumor cells. On the other hand, staining for ZO-1 was accentuated on the apical membrane of tumor cells that formed rosette structures and, at higher cell densities, was localized in the center of the rosettes (Fig. 2 j–l). There were no correlations between *N*-cadherin and ZO-1 expression ($R=0.13$, $p=0.28$) or *N*-cadherin localization (diffuse versus cell membrane) and ZO-1 expression ($p=0.43$).

The rate of *N*-cadherin positivity in most of the tumors exceeded that of ZO-1 positivity (Table 1). Comparison of immunoreactivity between *N*-cadherin and ZO-1 showed that their positivity rates were 55% versus 45% in pulmonary neuroendocrine tumors ($p=0.021$) and 83% versus 22% in other rosette-forming tumors ($p=0.03$), respectively. However, the rate of ZO-1 positivity in LCNEC of the lung tended to be higher than that of *N*-cadherin (52% vs 44%, $p=0.12$). Although the number of cases was limited, 100% of the immature teratomas examined were positive for both ZO-1 and *N*-cadherin (Table 1).

Table 1 *N*-cadherin and ZO-1 expression in all tumors with rosette structures

		No. of positive cases[b]		
	Total	*N*-cadherin	ZO-1	*p* Value
Pulmonary neuroendocrine tumors				
Typical carcinoid of the lung	5	4 (80%)	1 (20%)	0.068
Atypical carcinoid of the lung	2	1 (50%)	1 (50%)	0.66
LCNEC of the lung	25	11 (44%)	13 (52%)	0.12
Small cell carcinoma of the lung	8	5 (62.5%)	3 (37.5%)	0.043
	40	22 (55%)	18 (45%)	0.021
Other rosette-forming tumors				
Large cell carcinoma of the lung	2	2 (100%)	0 (0%)	0.16
Immature teratoma	2	2 (100%)	2 (100%)	0.18
Others[a]	14	11 (78.6%)	2 (14.3%)	0.008
	18	15 (83.3%)	4 (22.2%)	0.03

LCNEC large cell neuroendocrine carcinoma

[a] Others: ependymoma, mature teratoma, medulloblastoma, neuroblastoma, neurocytoma,olfactory neuroblastoma, pineoblastoma, retinoblastoma, and atypical carcinoid of the colon

[b] Positive cases are adopted if RoI is 5% or more

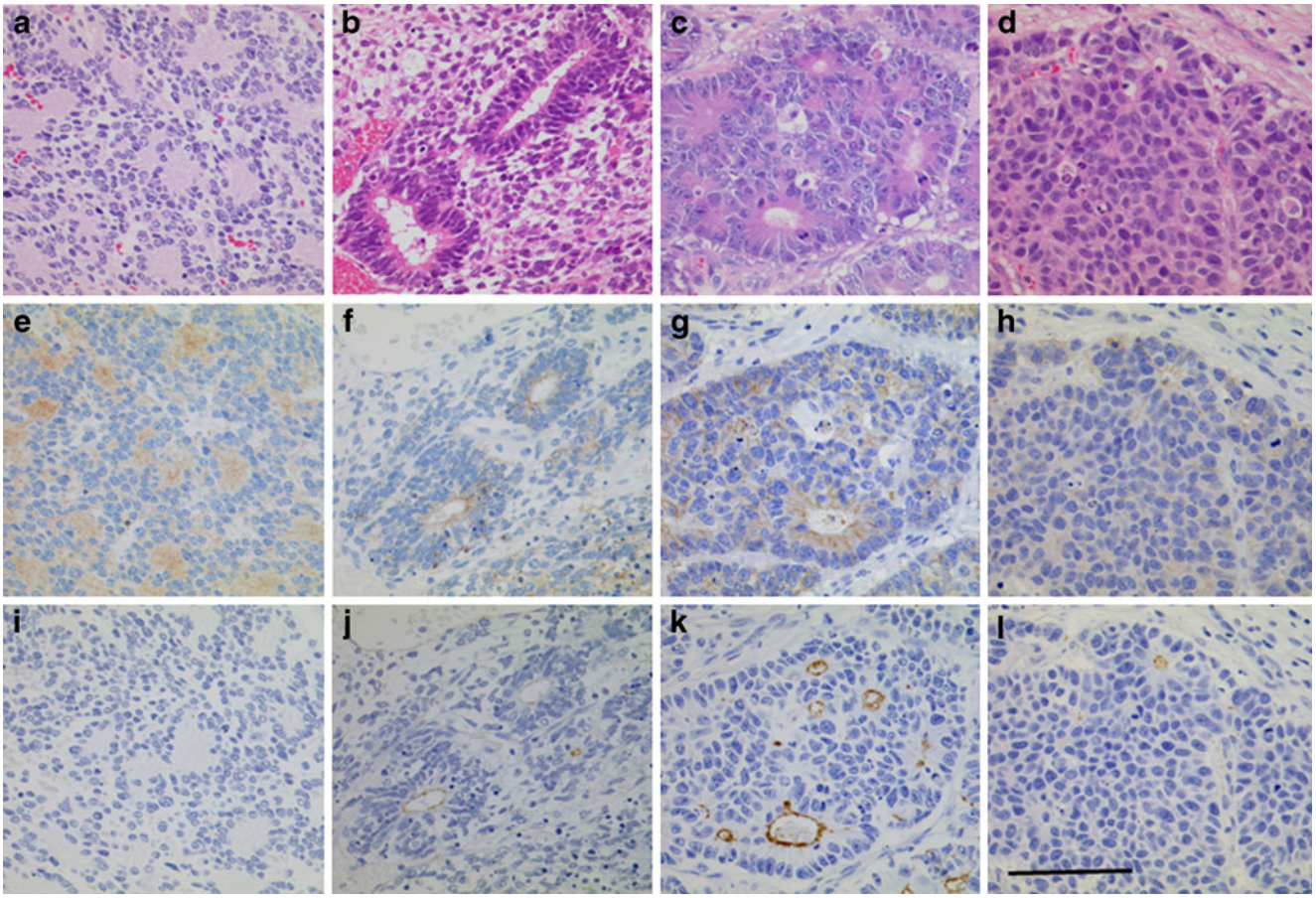

Fig. 2 Histological characterization of tumors with rosette structures. Neuroblastoma (**a**, **e**, **i**), immature teratoma (**b**, **f**, **j**), large cell neuroendocrine carcinoma of the lung (**c**, **g**, **k**), and small cell carcinoma of the lung (**d**, **h**, **l**) are shown. Immunoreactivity for *N*-cadherin (**e**, **f**, **g**, **h**) and ZO-1 (**i**, **j**, **k**, **l**) is shown. Scale *bar* is 100 μm

Histological features of rosette structures in neuroendocrine tumors

As mentioned in "Materials and methods," we found two patterns of rosette structure in neuroendocrine tumors: Flexner-type rosettes and Homer–Wright-type rosettes (Fig. 1). We divided pulmonary neuroendocrine tumors into two types: Flexner-type tumors (in which rosette structures with lumina were predominant) and Homer–Wright-type tumors (in which rosette structures without lumina were predominant). On this basis, 16 tumors were considered to be the Flexner-type and 24 were considered to be the Homer–Wright-type (Table 2). The Flexner-type tumors included one carcinoid tumor (1/7, 14.3%), 12 LCNECs (12/25, 48%), and three SCLCs (3/8, 37.5%). We then determined the RoI for both ZO-1 and *N*-cadherin. Flexner-type neuroendocrine tumors showed significantly higher values of RoI for ZO-1 than Homer–Wright-type neuroendocrine tumors (median, 38.8% vs 0%; 25th percentile, 19.3% vs 0%; 75th percentile, 55.5% vs 0%; $p<0.001$, respectively; Fig. 3). However, there were no significant differences of RoI between the two types of tumor for *N*-cadherin (median and mean, 52.2% vs 6.7% and 38.4% vs 24.6%, $p=0.387$, respectively; data not shown).

Table 2 Pathological diagnosis of Flexner-type and Homer–Wright-type pulmonary neuroendocrine tumors

Pulmonary neuroendocrine tumors	Number of tumors		
	Total	Flexner-type	Homer–Wright type
Typical carcinoid	5	0 (0%)	5 (100%)
Atypical carcinoid	2	1 (50%)	1 (50%)
LCNEC of the lung	25	12 (48%)	13 (52%)
Small cell carcinoma	8	3 (37.5%)	5 (62.5%)
	40	14 (35%)	26 (65%)

LCNEC large cell neuroendocrine carcinoma

Carcinomas with tubular structures

In order to examine the expression of ZO-1 and *N*-cadherin in tubular adenocarcinomas, in which it is sometimes difficult to discriminate rosettes from glandular structures,

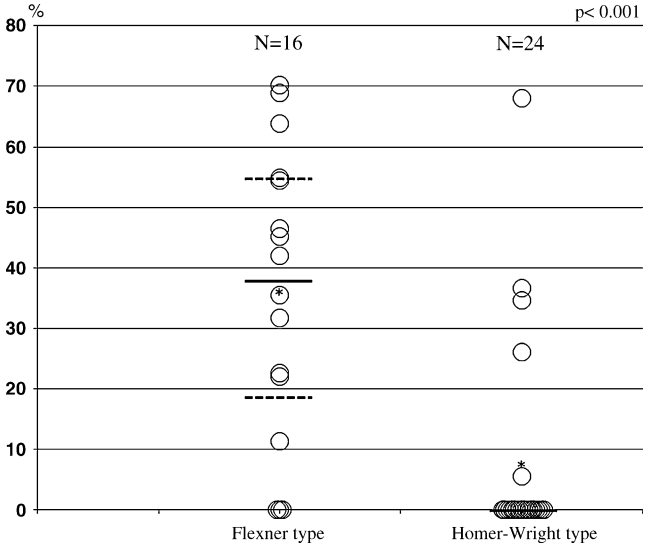

Fig. 3 ZO-1-positive rosette structures in neuroendocrine tumor of the lung (total 40 cases). Flexner-type tumors (in which rosette structures with lumina are predominant) showed significantly higher values of rosette index for ZO-1 than Homer–Wright-type tumors (in which rosette structures without lumina are predominant; $p<0.001$). *Asterisk*: mean; *solid line*: median; and *dashed line*: 25th and 75th percentiles, respectively. Statistical analysis was performed by *U* test

we assessed 43 well-differentiated tubular adenocarcinomas (described in "Materials and methods"; Fig. 4a–d). There was no positive staining for *N*-cadherin among adenocarcinomas of the lung (Fig. 4e), stomach (Fig. 4f), colon, pancreas (Fig. 4g), bile duct, and breast (Fig. 4h). All of the tubular adenocarcinomas were also negative for ZO-1 (Fig. 4 i–l), except for one ductal carcinoma of the breast (Fig. 4l, insert) in which the ductal structures were negative for other common neuroendocrine markers such as synaptophysin, chromogranin-A, and CD56/NCAM, although a few cases were positive for neuroendocrine markers (Table 3). Among ten tumors of the breast, one invasive ductal carcinoma was positive for ZO-1 and also for estrogen receptor and progesterone receptor, but negative for Her2 protein.

The immunoreactivities for both ZO-1(median and mean, 0% vs 0% and 0.23% vs 18%, $p<0.0001$) and *N*-cadherin (median and mean, 0% vs 0% and 0% vs 33% $p<0.0001$) differed significantly between adenocarcinoma and pulmonary neuroendocrine tumor.

Discussion

In this study, we demonstrated positive immunoreactivity for both *N*-cadherin and ZO-1 in neuroendocrine tumors showing rosette formation. It was of considerable interest that staining of the rosettes was similar to that of neural tube/neural rosettes in immature teratoma. These results indicated that both Flexner-type and Homer–Wright-type rosettes may mimic the neural tube in embryos, not only morphologically but also functionally. In tumors positive for ZO-1 and *N*-cadherin, ZO-1 positivity was localized in rosette structures, especially at the apical membrane of the constituent tumor cells, and the staining pattern was very rosette-specific, especially in Flexner-type tumors (Fig. 2). The correlation between ZO-1 and *N*-cadherin in Flexner-type tumors was significant ($R=0.595$, $p=0.004$). These results suggested that ZO-1 and *N*-cadherin are molecules playing a specific role in rosette morphology, not only in the neural tube but also pulmonary neuroendocrine tumor. In the early stage of neurogenesis, ZO-1 acts as a tight junction protein and regulates rosette growth to control symmetric versus asymmetric differentiation of neural stem cells. ZO-1 functions as a cross-linker between α-catenin and the actin cytoskeleton. The interaction between ZO-1 and *N*-cadherin is a key determinant of stable localization of both adherens junctions and gap junctions in the intercalated disks of rat myocytes, and expression of ZO-1 and *N*-cadherin, in relation to the so-called "cadherin switch", has also been reported in melanoma. The present study suggests that the former mechanism, regulating the turnover of stem cells, is more likely, although additional experimental studies to verify this possibility will be needed [27, 28].

There are two types of neuroendocrine markers: morphological markers such as rosette formation and palisading of the tumor cells, and immunohistochemical markers such as synaptophysin, chromogranin-A, and CD56/NCAM. These two marker types are frequently used for routine surgical diagnosis, but the relationship between them has not been studied in detail. In this study, we showed that ZO-1 and *N*-cadherin, which are specifically expressed in the neural tube, are characteristically expressed in the rosette structures of neuroendocrine tumors. Therefore, ZO-1 and *N*-cadherin are markers that are closely associated with neuroendocrine morphology and could be implicated in the formation of rosette structures.

Among the pulmonary neuroendocrine tumors, carcinoid tumor and SCLC are diagnosed on the basis of purely morphological criteria [2]. However, to diagnose LCNEC, positivity for an immunohistochemical marker (at least one among synaptophysin, chromogranin-A, and CD56/NCAM [2]) is required. These three neuroendocrine markers were considered to be useful for diagnosis of LCNEC. However, this set of immunohistochemical markers is provisional and is simply used empirically. We suggest that ZO-1 or *N*-cadherin could also be a useful marker of neuroendocrine differentiation and may be positive in cases of large cell carcinoma (LCC) with neuroendocrine morphology. LCC with neuroendocrine morphology mimics LCNEC but is negative for all three neuroendocrine markers. However, if

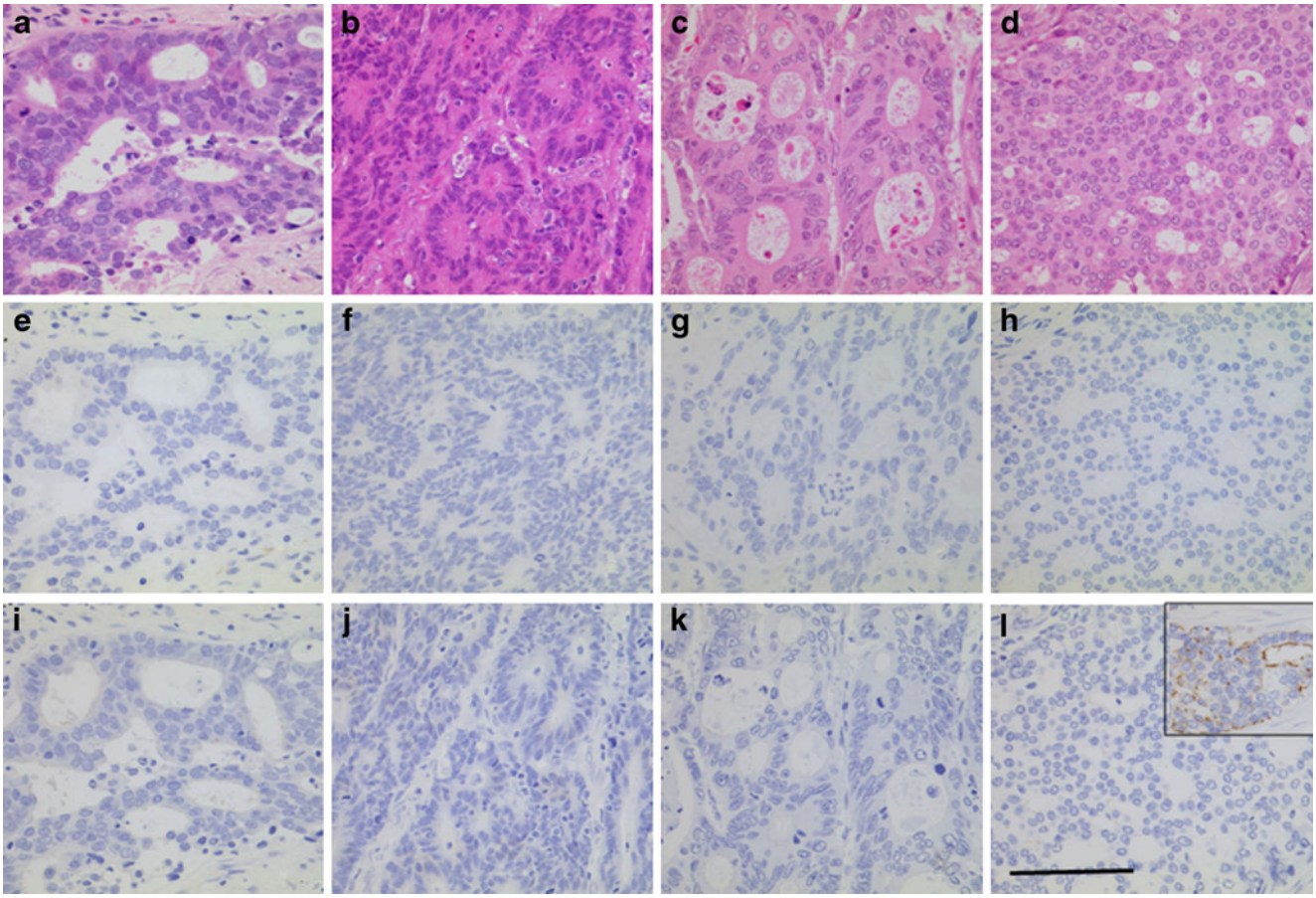

Fig. 4 Histological characterization of carcinomas with tubular structures. Lung adenocarcinoma (**a**, **e**, **i**), stomach adenocarcinoma (**b**, **f**, **j**), pancreas adenocarcinoma (**c**, **g**, **k**), and breast carcinoma (**d**, **h**, **l**) are shown. There is no immunoreactivity for *N*-cadherin (**e**, **f**, **g**, **h**) and ZO-1 (**i**, **j**, **k**, **l**). *Insert* is a ZO-1-positive area in invasive region of breast carcinoma in one of ten cases (**l**). Scale *bar* is 100 μm

positivity for ZO-1 and/or *N*-cadherin can be demonstrated, both LCNEC and LCC with neuroendocrine morphology may prove to be closely related tumors biologically and classifiable into a similar category.

SCLC and LCNEC are both high-grade neuroendocrine carcinomas of the lung. The present study demonstrated that a significantly higher proportion of SCLC cases (p= 0.043) were positive for *N*-cadherin than for ZO-1 and that more cases of typical carcinoid and atypical carcinoid (p= 0.068 and 0.66) were positive for *N*-cadherin than for ZO-1 (Table 1). Interestingly, however, the positivity rate for ZO-1 (52%) was relatively higher in LCNEC than in SCLC

Table 3 Immunohistochemical status of carcinomas with tubular structures

		No. of positive cases (%)				
	Total	Syn.	Ch-A.	CD56.	*N*-cadherin	ZO-1
Lung	3	1 (33%)	0 (0%)	0 (0%)	0 (0%)	0 (0%)
Stomach	10	2 (20%)	0 (0%)	0 (0%)	0 (0%)	0 (0%)
Colon	10	1 (10%)	0 (0%)	0 (0%)	0 (0%)	0 (0%)
Pancreas/bile duct	10	0 (0%)	0 (0%)	0 (0%)	0 (0%)	0 (0%)
Breast	10	1 (10%)	1[a] (10%)	1[a] (10%)	0 (0%)	1 (10%)

The percentage values are rounded to the nearest whole number

Syn synaptophysin, *Ch-A* chromogranin-A, *CD56* CD56/NCAM

[a] Positivity for both was recognized in an identical case and was positive for estrogen receptor and progesterone receptor, but negative for Her2 protein. This case was diagnosed as primary ductal carcinoma with neuroendocrine features since the case did not show specific neuroendocrine morphological findings and had intraductal carcinoma component

(37.5%) or carcinoid tumor (28.6%; Table 1). This difference may have been attributable to the rosette subtypes present. SCLC and carcinoid tumors frequently include Homer–Wright-type rosettes, which express ZO-1 less frequently than Flexner-type rosettes (Table 2 and Fig. 3). These results indicate that LCNEC is more closely associated with neural tube formation than is the case for SCLC and suggest that these two high-grade neuroendocrine carcinomas of the lung originate from different cells, and/or have different mechanisms of carcinogenesis.

In order to compare the immunohistochemical characteristics of rosettes and tube-like structures, we examined 43 well-differentiated tubular adenocarcinomas for their expression of ZO-1 and *N*-cadherin. Almost all cases were negative for both ZO-1 and *N*-cadherin (Fig. 4 and Table 3). This was not surprising because the tubular structures of adenocarcinoma are not rosettes and would thus be nearly negative for both proteins. The present results indicated that ZO-1 and *N*-cadherin would be very powerful immunohistochemical markers for differentiating rosettes from tubular structures in adenocarcinoma. On the other hand, it was interesting to note that one ductal carcinoma of the breast (1/43, 2.3%) expressed ZO-1 strongly in the apical area of tubular structures only in the invasive area (RoI=32.3%), the staining pattern being similar to that of Flexner-type rosettes (Fig. 4**l**, insert). However, this case was negative for other markers of neuroendocrine differentiation (synaptophysin, chromogranin-A, and CD56/NCAM). Therefore, the biological significance of ZO-1 may differ from that of other common neuroendocrine markers.

To our knowledge, this is the first report to have pointed out the similarity between rosette structures in pulmonary neuroendocrine tumors and the embryonic neural tube. Although this study is descriptive and preliminary, our findings allow us to propose a completely original concept that will undoubtedly be helpful for understanding the mechanisms leading to rosette formation in neuroendocrine tumors, recapitulating formation of the neural tube during embryogenesis. On the basis of these results, we propose that ZO-1 and *N*-cadherin are very useful immunohistochemical markers of rosettes in pulmonary neuroendocrine tumors, allowing them to be differentiated from glandular structures in adenocarcinoma, especially in small specimens. This knowledge may be of help in understanding the biological features of pulmonary neuroendocrine tumor and the essential differences between LCNEC and SCLC.

Since the number of cases examined here was limited, we did not analyze the outcome of the studied patients. Therefore, it will be necessary to confirm the outcome in a prospective study using a large cohort. A few previous studies have examined the contribution of ZO-1 to prognosis. Their findings have indicated that the level of ZO-1 messenger RNA is a valuable indicator of outcome in patients with non-small cell lung cancer and that there is no significant correlation between the level of ZO-1 immunoexpression and outcome in gastric cancer [29] [30]. On the other hand, Asamura et al. have reported that the diagnosis of LCNEC is a predictor of poor outcome [31]. It would be interesting to analyze the outcome of cases of large cell carcinoma lacking expression of synaptophysin, chromogranin-A, and CD56/NCAM, but showing ZO-1- and *N*-cadherin-positive rosette formation, which until now have not been classified as LCNEC.

In conclusion, analysis of ZO-1 and *N*-cadherin may help to clarify the mechanisms leading to rosette formation in neuroendocrine tumors, in the context of neural tube formation during embryogenesis, and may have utility in the diagnosis of pulmonary neuroendocrine tumors in differentiating rosettes from glandular structures in adenocarcinoma, especially in small specimens.

Conflict of interest statement We declare that we have no conflicts of interest.

References

1. Colby TV KM, Travis WD. Large cell neuroendocrine carcinoma:, In: Colby TV KM, Travis WD, editors (1995) Tumors of the lower respiratory tract. Armed Forces Institute of Pathology:248–257
2. Travis WD BE, Müller-Hermelink HK, Harris CC editor (2004) Pathology and Genetics of Tumours of the Lung, Pleura, Thymus and Heart. World Health Organization Classification of Tumours 10
3. Arrigoni MG, Woolner LB, Bernatz PE (1972) Atypical carcinoid tumors of the lung. J Thorac Cardiovasc Surg 64(3):413–421
4. Carretta A, Ceresoli GL, Arrigoni G, Canneto B, Reni M, Cigala C, Zannini P (2000) Diagnostic and therapeutic management of neuroendocrine lung tumors: a clinical study of 44 cases. Lung Cancer 29(3):217–225
5. Garcia-Yuste M, Matilla JM, Alvarez-Gago T, Duque JL, Heras F, Cerezal LJ, Ramos G (2000) Prognostic factors in neuroendocrine lung tumors: a Spanish Multicenter Study. Spanish Multicenter Study of Neuroendocrine Tumors of the Lung of the Spanish Society of Pneumonology and Thoracic Surgery (EMETNE-SEPAR). Ann Thorac Surg 70(1):258–263
6. Gould VE, Linnoila RI, Memoli VA, Warren WH (1983) Neuroendocrine cells and neuroendocrine neoplasms of the lung. Pathol Annu 18(Pt 1):287–330
7. Jiang SX, Kameya T, Shoji M, Dobashi Y, Shinada J, Yoshimura H (1998) Large cell neuroendocrine carcinoma of the lung: a histologic and immunohistochemical study of 22 cases. Am J Surg Pathol 22(5):526–537
8. Naranjo Gomez JM, Gomez Roman JJ Behaviour and survival of high-grade neuroendocrine carcinomas of the lung. Respir Med 104 (12):1929–1936
9. Peng WX, Sano T, Oyama T, Kawashima O, Nakajima T (2005) Large cell neuroendocrine carcinoma of the lung: a comparison with large cell carcinoma with neuroendocrine morphology and small cell carcinoma. Lung Cancer 47(2):225–233
10. Takei H, Asamura H, Maeshima A, Suzuki K, Kondo H, Niki T, Yamada T, Tsuchiya R, Matsuno Y (2002) Large cell neuroendocrine carcinoma of the lung: a clinicopathologic study of eighty-seven cases. J Thorac Cardiovasc Surg 124(2):285–292

11. Warren WH, Faber LP, Gould VE (1989) Neuroendocrine neoplasms of the lung. A clinicopathologic update. J Thorac Cardiovasc Surg 98 (3):321–332
12. Warren WH, Gould VE, Faber LP, Kittle CF, Memoli VA (1985) Neuroendocrine neoplasms of the bronchopulmonary tract. A classification of the spectrum of carcinoid to small cell carcinoma and intervening variants. J Thorac Cardiovasc Surg 89(6):819–825
13. Warren WH, Memoli VA, Gould VE (1988) Well differentiated and small cell neuroendocrine carcinomas of the lung. Two related but distinct clinicopathologic entities. Virchows Arch B Cell Pathol Incl Mol Pathol 55(5):299–310
14. Kloppel G (2007) Tumour biology and histopathology of neuroendocrine tumours. Best Pract Res Clin Endocrinol Metab 21(1):15–31
15. Wippold FJ 2nd, Perry A (2006) Neuropathology for the neuroradiologist: rosettes and pseudorosettes. AJNR Am J Neuroradiol 27(3):488–492
16. Koch P, Opitz T, Steinbeck JA, Ladewig J, Brustle O (2009) A rosette-type, self-renewing human ES cell-derived neural stem cell with potential for in vitro instruction and synaptic integration. Proc Natl Acad Sci U S A 106(9):3225–3230
17. Elkabetz Y, Panagiotakos G, Al Shamy G, Socci ND, Tabar V, Studer L (2008) Human ES cell-derived neural rosettes reveal a functionally distinct early neural stem cell stage. Genes Dev 22 (2):152–165
18. Aaku-Saraste E, Hellwig A, Huttner WB (1996) Loss of occludin and functional tight junctions, but not ZO-1, during neural tube closure–remodeling of the neuroepithelium prior to neurogenesis. Dev Biol 180(2):664–679
19. Nishimura T, Takeichi M (2008) Shroom3-mediated recruitment of Rho kinases to the apical cell junctions regulates epithelial and neuroepithelial planar remodeling. Development 135(8):1493–1502
20. Hatta K, Takeichi M (1986) Expression of N-cadherin adhesion molecules associated with early morphogenetic events in chick development. Nature 320(6061):447–449
21. Hatta K, Takagi S, Fujisawa H, Takeichi M (1987) Spatial and temporal expression pattern of N-cadherin cell adhesion molecules correlated with morphogenetic processes of chicken embryos. Dev Biol 120(1):215–227
22. Zynger DL, Dimov ND, Ho LC, Laskin WB, Yeldandi AV (2008) Differential expression of neural-cadherin in pulmonary epithelial tumours. Histopathology 52(3):348–354
23. Stevenson BR, Siliciano JD, Mooseker MS, Goodenough DA (1986) Identification of ZO-1: a high molecular weight polypeptide associated with the tight junction (zonula occludens) in a variety of epithelia. J Cell Biol 103(3):755–766
24. Itoh M, Nagafuchi A, Yonemura S, Kitani-Yasuda T, Tsukita S, Tsukita S (1993) The 220-kD protein colocalizing with cadherins in non-epithelial cells is identical to ZO-1, a tight junction-associated protein in epithelial cells: cDNA cloning and immunoelectron microscopy. J Cell Biol 121(3):491–502
25. Tsukita S, Yamazaki Y, Katsuno T, Tamura A, Tsukita S (2008) Tight junction-based epithelial microenvironment and cell proliferation. Oncogene 27(55):6930–6938
26. Katsuno T, Umeda K, Matsui T, Hata M, Tamura A, Itoh M, Takeuchi K, Fujimori T, Nabeshima Y, Noda T, Tsukita S, Tsukita S (2008) Deficiency of zonula occludens-1 causes embryonic lethal phenotype associated with defected yolk sac angiogenesis and apoptosis of embryonic cells. Mol Biol Cell 19(6):2465–2475
27. Palatinus JA, O'Quinn MP, Barker RJ, Harris BS, Jourdan J, Gourdie RG ZO-1 determines adherens and gap junction localization at intercalated disks. Am J Physiol Heart Circ Physiol 300 (2):H583-594
28. Smalley KS, Brafford P, Haass NK, Brandner JM, Brown E, Herlyn M (2005) Up-regulated expression of zonula occludens protein-1 in human melanoma associates with N-cadherin and contributes to invasion and adhesion. Am J Pathol 166(5):1541–1554
29. Wang Y, Zhou J, Zeng F, Huang Y, Zhou S, Liu X [Expression and clinical significance of ZO-1 in patients with non-small cell lung cancer]. Zhongguo Fei Ai Za Zhi 14 (2):146–150
30. Ohtani S, Terashima M, Satoh J, Soeta N, Saze Z, Kashimura S, Ohsuka F, Hoshino Y, Kogure M, Gotoh M (2009) Expression of tight-junction-associated proteins in human gastric cancer: down-regulation of claudin-4 correlates with tumor aggressiveness and survival. Gastric Cancer 12(1):43–51
31. Asamura H, Kameya T, Matsuno Y, Noguchi M, Tada H, Ishikawa Y, Yokose T, Jiang SX, Inoue T, Nakagawa K, Tajima K, Nagai K (2006) Neuroendocrine neoplasms of the lung: a prognostic spectrum. J Clin Oncol 24(1):70–76